ELSEVIER

Journal of Hazardous Materials B121 (2005) 89–108

Journal of Hazardous Materials

www.elsevier.com/locate/jhazmat

A hybrid liquid-phase precipitation (LPP) process in conjunction with membrane distillation (MD) for the treatment of the INEEL sodium-bearing liquid waste

M.S.H. Bader*

Bader Engineering and Laboratory, Inc., P.O. 10675, College Station, TX 77842, USA

Received 29 November 2004; received in revised form 24 January 2005; accepted 30 January 2005
Available online 5 March 2005

Abstract

A novel hybrid system combining liquid-phase precipitation (LPP) and membrane distillation (MD) is integrated for the treatment of the INEEL sodium-bearing liquid waste. The integrated system provides a "full separation" approach that consists of three main processing stages. The first stage is focused on the separation and recovery of nitric acid from the bulk of the waste stream using vacuum membrane distillation (VMD). In the second stage, polyvalent cations (mainly TRU elements and their fission products except cesium along with aluminum and other toxic metals) are separated from the bulk of monovalent anions and cations (dominantly sodium nitrate) by a front-end LPP. In the third stage, MD is used first to concentrate sodium nitrate to near saturation followed by a rear-end LPP to precipitate and separate sodium nitrate along with the remaining minor species from the bulk of the aqueous phase. The LPP–MD hybrid system uses a small amount of an additive and energy to carry out the treatment, addresses multiple critical species, extracts an economic value from some of waste species, generates minimal waste with suitable disposal paths, and offers rapid deployment. As such, the LPP–MD could be a valuable tool for multiple needs across the DOE complex where no effective or economic alternatives are available.

Keywords: Precipitation; Membrane distillation; INEEL sodium-bearing waste; Toxic metals; TRU elements and fission products

1. Introduction

The Idaho Nuclear Technology and Engineering facility (INTEC) located at the Idaho National Engineering and Environmental Laboratory (INEEL) site was established in the early 1950s to store and reprocess spent nuclear fuel for the recovery of uranium-235. Most reprocessing was performed on aluminum- or zirconium-clad uranium fuels [1]. Smaller quantities of stainless steel and graphite clad uranium fuels were also reprocessed. The INEEL tanks waste contains: (1) predominately nitric acid, nitrate, and sodium; (2) significant amounts of aluminum (or zirconium), and potassium; (3) appreciable amounts of sulfates, phosphates, chlorides, and toxic metals (chromium, mercury, iron, lead, nickel, and manganese); and (4) small amounts of Transuranic (TRU) elements (plutonium, neptunium, americium, and curium) and their fission products (cesium, strontium and barium) [1].

The INEEL tanks waste is uniquely different from most tanks waste at other DOE sites (e.g., Hanford, Savannah River, and Oak Ridge) [1]. The INEEL waste is extremely acidic, while most tanks waste at other sites is very basic. The basicity of tanks waste in other DOE sites has caused many inorganic species to segregate into complex mixtures of liquids, slurries, and sludges. In contrast, inorganic species remain dissolved in the INEEL acidic tanks waste (the liquid is clear almost to the bottom of the tanks) [1].

The INEEL liquid waste has been divided into high-activity waste (HAW), and sodium-bearing liquid waste. All of the HAW resulting from the dissolution and processing of spent nuclear fuel has been calcined and stored in stainless

* Tel.: +1 979 680 8000; fax: +1 979 680 8007.
E-mail address: manny@baderinc.com.
URL: http://www.baderinc.com.

0304-3894/$ – see front matter © 2005 Elsevier B.V. All rights reserved.
doi:10.1016/j.jhazmat.2005.01.017

Nomenclature

%AAD	percent average absolute deviation
C_F	MD bulk feed concentration
C_i	model's interaction parameters
C_m	MD feed concentration at the membrane surface
$C_{1,m}$	concentration of salt species in filtered sample
$C_{1,2}$	concentration of salt species in standard sample
J	permeate flux through MD or VMD membrane
M_i	molar concentration of individual ions
NP	number of points
p^s	vapor pressure of the aqueous solution
p^0	vapor pressure of pure water
P	precipitation fraction
R	ideal gas constant
RMSE	root mean square error
SS	objective function
T	temperature
T_F	MD feed temperature
T_{Fm}	MD bulk feed temperature at the membrane surface
T_P	MD bulk permeate temperature
T_{Pm}	MD permeate temperature at the membrane surface
v_i	molar volume of solvent i
v_w	water molar volume
V_r	solvents volume ratio (organic/water)
V_i	volume of solvent i
$x_{i,j}$	mole fraction (solubility) of species i in solvent j
$x_{i,m}$	mole fraction (solubility) of species i in mixed-solvents mixture m

Greek letters

θ_i	volume fraction of solvent i
Λ_1	salt binary-solvent interaction parameter (ternary constant)
$\Lambda_{i,j}$	interaction parameter of solvent i with solvent j
Π	osmotic pressure

Subscripts

Cal	calculated
Exp	experimental
m	mixed-solvent mixture
w	water
1	salt species
2	water solvent
3	organic solvent

Superscripts

E	excess
s	solution
0	pure

steel bin sets enclosed in concrete vaults with walls up to four feet thick (interim storage). However, the sodium-bearing liquid waste still remains in storage tanks.

In the calcination process, a fluidized bed is operated at about 500 °C to convert liquid waste (evaporates water, nitric acid, and volatile species) into a dry granular solid composed mainly of metal oxides [2]. The average weight percentages of the main constituents in the calcined waste from aluminum-clad fuels are: 91% aluminum oxide; 3% sodium oxide; 1% iron oxide; 1% boron oxide; 1% sulfate; and less than 1% fission product oxides [2]. However, the average weight percentages of the main constituents in the calcined waste from zirconium-clad fuels are: 54% calcium fluoride; 24% zirconium oxide; 14% aluminum oxide; 4% calcium oxide; 3% boron oxide; and less than 1% fission product oxides [2].

The use of the calcination process is attributed to two main factors. The first factor is that the volume of the calcine waste is about seven times less than the volume of the liquid waste. The second factor is that the calcine waste is more chemically stable than the liquid waste. Thus, it is to some extent safer to store than the liquid waste. However, significant operational problems were associated with the calcination of the INEEL waste.

First, the significant presence of alkali cations (sodium and potassium) in the feed leads to form nitrate complexes that melt at temperatures below 500 °C, and agglomerate the calcine in the fluidized bed (loss of fluidization) [2]. To solve this problem, large amounts of aluminum nitrate must be added to dilute the concentrations of sodium and potassium to levels that would not affect the operation of the fluidized bed. This would reduce the overall process efficiency, and would lead to lower the depletion rate of the tanks waste (the net liquid volume to solid volume is reduced from 7 to 2). In fact, the division of the INEEL waste into HAW and sodium-bearing liquid waste is, to a large extent, attributed to this problem. As a result, it is anticipated that the remaining INEEL sodium-bearing liquid waste is unlikely to be calcined before 2012, as required by the settlement agreement (the State of Idaho, DOE and Navy) [1,2].

Second, to apply the calcination process to the remaining sodium-bearing liquid waste, it was suggested that the fluidized bed ought to be operated at higher temperatures to decompose some of the alkali cations without the addition of excessive amounts of aluminum nitrate [2]. A laboratory-scale study indicated that a feed composition with a 1.5–1.0 molar ratio of aluminum to alkali cations can be calcined at 600 °C [2]. This represents a 60% reduction in the amount of aluminum (3.1–1.0 molar ratio of aluminum to alkali cations) that must be added to the calciner feed at 500 °C (baseline operation). However, the application of the Maximum Achievable Control Technology (MACT) rule requires significant off-gas treatment and monitoring for carbon monoxide, NO*x*, and products of incomplete combustion. In addition, the operation of the calcination process at higher temperatures is more energy intensive.

Third, many radionuclides and hazardous species can be easily leached out from the high-activity calcined waste. This stems from the designed chemistry of the calcination process in which calcine materials could be dissolved in nitric acid to allow for periodic clean out of the calciner vessel and off-gas systems [2]. As such, the calcined waste is an interim form of waste that is not acceptable for permanent disposal. Thus, it requires further treatment for final immobilization and isolation of radioactive and toxic species from the environment.

Fourth, hydrofluoric acid was used to dissolve zirconium-clad uranium fuels. The use of hydrofluoric acid generated large amounts of fluoride in the fluidized bed. As a result, substantial amounts of calcium nitrate were added to inhibit fluoride volatility, and to reduce corrosion of the fluidized bed vessel and off-gas systems [2].

The DOE environmental restoration strategy for the INEEL site to treat both the sodium-bearing liquid waste and high-activity calcined waste can be seen in four overall possible treatment options. The first option is to calcine the remaining sodium-bearing liquid waste, and then leave the "total calcine waste" in the interim solid storage facilities [2]. The term "total calcine waste" refers to the sodium-bearing calcine waste plus the already existed high-activity calcined waste. This option is based on the assumption that over time, the "total calcine waste" will lose most of its radioactivity as a result of the decay of mainly the fission products, cesium (Cs-137) and strontium (Sr-90). While the half-lives of Cs-137 and Sr-90 are 30 and 29 years, respectively, the half-lives of TRU elements (plutonium, neptunium, americium, and curium) range from a few hundred years to several thousand years. As such, it is highly anticipated that this "no action option" will not meet all of the requirements of the Settlement Agreement or current environmental regulations.

The second option is to calcine the remaining sodium-bearing liquid waste, and then convert the "total calcine waste" to a final immobilized waste form by direct immobilization. However, the direct immobilization of the "total calcine waste" will be extremely expensive. Vitrification, the process of converting materials into a glass-like substance, is the baseline immobilization method. The estimated cost of vitrification and repository is about $1 million per glass canister (1650 kg) [3]. Cost reduction in the vitrification process can only occur through selective removal of targeted high-activity species from waste (less than 1 wt.% of the total calcine waste) to reduce the number of glass canisters produced and to improve process efficiency.

The third option is to calcine the remaining sodium-bearing liquid waste, and then to redissolve the "total calcine waste" in nitric acid. Radioactive species (high-activity) will then be separated from the bulk of the dissolved "total calcine waste" for final immobilization. This option requires a sequence of separation processes to partition the dissolved "total calcine waste" mainly into a small volume of high-level waste (HLW) for deep geologic disposal and a larger volume of low-level waste (LLW) for burial in near-surface facilities. This allows the higher cost vitrification facility to be scaled down in size, reducing both long-term capital and operating costs. The disadvantages of this option, however, are: (1) the use of the inefficient calcination process (high energy consumption, addition of significant amounts of chemicals, off-gas treatment, etc.); and (2) the generation of a temporary waste form (sodium-bearing calcine waste) that must be stored, re-dissolved, and reprocessed again (long-term cost).

The fourth option is to: (1) separate radioactive species from the bulk of the remaining sodium-bearing liquid waste; and (2) re-dissolve the high-activity calcined waste in nitric acid for the purpose of selective separation of radioactive species. This option is probably the most appropriate one that could lead to subsequent immobilization of high- and low-activity waste fractions, and minimization of the vitrification cost. Unlike the first three options in which existing processing facility to calcine (if successful) the remaining sodium-bearing liquid waste will be used, this option eliminates the need for using the calcination process. However, this option requires substantial capital expenditures in the near-term time frame.

Due to toxicity, radioactivity, and sheer volumes of such waste, a processing system could be successful only if it: (1) uses a very small amount of additives and energy to carry out the treatment; (2) addresses multiple critical substances rather than a single one; (3) can be applied where no reliable or economic alternatives are available; (4) generates minimal waste with suitable disposal paths; and (5) offers rapid deployment. Several solvent extraction processes to selectively separate TRU elements and their fission products from the bulk of the acidic waste have been proposed and extensively tested at the INEEL facility [see e.g. 4–8]. However, more innovative technologies ought to be sought to treat the INEEL sodium-bearing liquid waste as well as the high-activity calcined waste that will be dissolved in the future for further processing. In addition, there is a need to re-evaluate the entire INEEL waste treatment options in terms of processing efficiency, and environmental responsibility with incentives of conducive economics.

A liquid-phase precipitation (LPP) in conjunction with membrane distillation (MD) were integrated in a hybrid system to potentially treat the INEEL sodium-bearing liquid waste. The objectives of this work were to: (1) demonstrate the technical feasibility of the LPP for the segregation of inorganic species from a simulated INEEL sodium-bearing liquid waste, and (2) assess the integration of the hybrid LPP–MD for the treatment of the INEEL sodium-bearing liquid waste.

2. Processing concepts

2.1. Liquid-phase precipitation (LPP)

Unlike conventional precipitation approaches, the LPP involves the addition of a non-hazardous, miscible precipitation solvent that can be nearly completely recovered [9,10]. The effect of the separation in the LPP is to intermix an aqueous

solution with a suitable amine solvent at ambient temperature and atmospheric pressure to form selective precipitates. The suitable amine solvents are those which have the ability to meet two basic criteria: (1) suitability to precipitate targeted inorganic species from aqueous solutions; and (2) suitability for overall process design. The selected amine solvent must be miscible with the aqueous phase. Of equal importance, the targeted inorganic species must be sparingly soluble (preferably nearly insoluble) in the amine solvent.

For ease of recovery and reuse, the selected amine solvent must have favorable physical properties such as low boiling point, and no azeotrope formation with water. From a process design standpoint, the selected amine must have low toxicity since traces always remain in the discharge stream. In addition, the selected amine must be chemically stable, compatible with the process, and relatively inexpensive. Several amines have been identified for potential use in the LPP process. These amines are isopropylamine (IPA), propylamine (PA), diisopropylamine (DIPA), ethylamine (EA), diethylamine (DEA), methylamine (MA), and dimethylamine (DMA). However, IPA is the most favorable amine solvent [11–14].

The effectiveness of the LPP process is based on the fact that a solid phase will form or re-form if a targeted dissolved inorganic solute in a solvent environment is elevated from sub-saturation to higher concentrations (e.g., near-saturation). The addition of an amine solvent to an inorganic–aqueous solution leads to the capture of part of the water molecules and reduces the aqueous solubility of the inorganic solute to form insoluble precipitates. The ionic charge, the ionic radius, the presence of sufficient and suitable anionic and cationic species, and the solubility limits of the targeted cationic–anionic compound in both water and amine solvents play an important role in the degree of forming precipitates. As such, the amount of the added amine for effective precipitation determines the economical value of the LPP process.

In applications where a targeted dissolved inorganic species has appreciable aqueous solubility limit, the effectiveness of the LPP as a stand-alone process is limited. For instance, the selective removal of alkali cations (sodium, potassium, and cesium) or monovalent anions (e.g., nitrate and chloride) or even divalent anions such as sulfate (at low concentrations or in the absence of sparingly soluble alkaline cations), can be enhanced if the LPP process is modified with a pre-concentration step to elevate the concentration of such species [15,16]. A pre-concentration processing step is also needed to efficiently minimize the use of the amine solvent. Membrane distillation (MD) can serve as a pre-concentration step for the LPP.

2.2. Membrane distillation (MD)

MD refers to the transport of the vapor phase through pores of a hydrophobic membrane that separates two liquid solutions. The liquid solution cannot enter the membrane pores unless the applied pressure is greater than the specified "liquid entry" pressure (less than 45 psi) for the porous partition of a given membrane. In the absence of such a pressure, vapor–liquid interfaces are formed on both sides of the membrane pores due to surface tension forces. Under these conditions, if a temperature difference is applied, a vapor pressure gradient will be created on both interfaces. Evaporation will take place at the warm membrane interface (feed), vapor will transport through the membrane pores with a convective and/or diffusion mechanism, and condensation will take place at the cold membrane interface (permeate). Thus, the net permeate vapor flux will be from the warm solution to the cold solution.

Several advantages of MD compared to conventional pressure-driven membrane or evaporation processes can be seen. First, MD can take place at sub-atmospheric or atmospheric pressures, and at temperatures that are significantly lower than the boiling point of water (e.g., 45–65 °C). Any form of waste heat (e.g., existing low temperature gradients typically available in processing plants) or low grade energy sources (wind or solar or geothermal) can be employed. A simple wind generator or a solar collector combined with a shell and tube heat exchange can be used to operate MD system. It should be pointed out that the wide variations in the temperatures of some of the DOE tanks waste (approach 93 °C) can also be used to operate MD. Second, the distillate product from an aqueous stream containing non-volatile inorganics is an ultra-pure, and thus entrainment of dissolved inorganics in the product stream, as the case with pressure-driven membranes, is avoided. Third, the evaporation surface of MD can be made similar to the available various pressure-driven membrane modules (e.g., hollow fiber, spiral wound, etc.). Such a modularity of MD allows the addition of processing capacity as needed, flexibility and simplicity not available with conventional evaporation processes. Fourth, design issues such as mist, scaling, corrosion, and foaming are minimal.

MD can be evaluated in terms of the permeate vapor flux as a function of the: (1) differences in temperatures and vapor pressures (feed and permeate streams); (2) inorganic concentrations in the feed stream; and (3) tangential velocity (flow rate). Since the INEEL sodium-bearing liquid waste is a highly concentrated stream, the apparent simplicity of MD could obscure complex and simultaneous heat and mass transfer interactions. A progressive increase in inorganic concentrations on the feed side of MD could dramatically reduce, if not completely cease or even reverse the permeate vapor flux. The vapor and osmotic pressures are directly related to inorganic concentrations in the stream. When the aqueous solubilities limits of targeted inorganic species are very high, and as evaporation takes place, the viscosity of the solution will increase (decrease mass transfer) with the increase of inorganic concentrations. This would lead to significantly depress the permeate vapor pressure across the membrane, and elevate the solution osmotic pressure. Controlling inorganic concentrations in the feed stream is a critical factor

equivalent to inducing and controlling the temperature as a driving force between the feed and permeate streams. Hence, the practicality of MD hinges on its ability to provide a steady and acceptable rate of permeate vapor flux.

Vacuum membrane distillation (VMD) is identical to MD except that the permeate pressure is lowered below the equilibrium vapor pressure by vacuum. Condensation of the permeate takes place outside the membrane module. VMD is thus an equilibrium-based process where the employed thin porous hydrophobic membrane does not interfere with the selectivity of the vapor–liquid equilibrium. When vapor–liquid equilibrium is favorable, the permeate flux in VMD is therefore expected to be large. VMD can be used to recover volatile species such as the LPP precipitation solvent (IPA), or nitric acid from the INEEL sodium-bearing liquid waste.

3. Experimental

The average concentrations profile of the INEEL sodium-bearing liquid waste is given in Table 1 [4]. We have referred cations and anions to their possible basic compounds. The compounds were then divided into five groups (nitrate, phosphate, sulfate, fluoride, and chloride). The nitrate group, which is the dominant anion in the INEEL sodium-bearing liquid stream, contains all cations, while the rest of the groups are only in the form of sodium. Recipes of such compounds were used to prepare a stock aqueous solution representing the average inactive INEEL sodium-bearing liquid waste.

Inspection of Table 1 reveals that the reported concentrations of the total anions (meq/L) are significantly higher than the concentrations of the total cations (meq/L). Such an imbalance in the total anions versus the total cations is attributed to the nitrate excess concentration. This can be explained by the fact that the INEEL sodium-bearing liquid waste is composed predominately of nitric acid and sodium nitrate. Nitric acid completely dissociates in water to produce hydrogen and nitrate. This would increase the concentration of nitrate in the reported INEEL sodium-bearing liquid waste. As such, in our simulated INEEL sodium-bearing liquid waste, the reported concentration of nitrate was reduced from 367,069 mg/L (5.92 M) [4] to 242,512 mg/L (3.91 M) to balance the total anions (4146.5 meq/L) against the total cations (4146.5 meq/L). It should be noted that the simulated INEEL sodium-bearing liquid waste was purposely spiked with a 100 mg/L of strontium (instead of the actual 1.18 mg/L), and a 100 mg/L of barium (instead of the 7.76 mg/L) for better analytical results. Europium (1063.7 mg/L or 0.007 M) was also added as a surrogate for americium [4].

Seven samples, each of which consists of 20 mL, were drawn from the simulated INEEL sodium-bearing stock solution and loaded into 100 mL flasks. One sample was used as a reference, and the remaining six samples were used to study the precipitation of the targeted species in the presence of different amounts of IPA. Different amounts of IPA (0.5, 1.0, 2.0, 4.0, 8.0, and 16.0 mL) were then drawn and injected into each of the six 20 mL samples. The pH values for each sample were measured (Orion-230A pH meter).

Table 1
A simulant profile for the INEEL sodium-bearing liquid waste

Species	Concentration	
	(mg/L)	(mol/L)
Cations		
Na	41841.00	1.82E00
K	7429.00	1.90E−1
Cs	3.84	2.89E−5
Ca	1844.00	4.60E−2
Sr	1.18	1.35E−5
Ba	7.76	5.65E−5
Hg	320.94	1.60E−3
Pb	414.40	2.00E−3
Mn	714.19	1.30E−2
Ni	117.38	2.00E−3
Al	16998.00	6.30E−1
Cr	208.00	4.00E−3
Fe	1228.63	2.20E−2
Eu	1063.72	7.00E−3
Zr	547.32	6.00E−3
Anions		
F	1273.00	6.70E−2
Cl	1205.00	3.40E−2
NO_3	367069.00	5.92E00
PO_4	1519.54	1.60E−2
SO_4	4898.94	5.10E−2

Compound	Concentration (mg/L)
Group 1—nitrate	
$NaNO_3$	134709.15
KNO_3	19209.00
$CsNO_3$	146.18
$Ca(NO_3)_2{\cdot}4H_2O$	10862.90
$Sr(NO_3)_2$	241.26
$Ba(NO_3)_2$	190.79
$Mn(NO_3)_2{\cdot}xH_2O$	2326.35
$Ni(NO_3)_2{\cdot}6H_2O$	581.62
$Al(NO_3)_3{\cdot}9H_2O$	236344.50
$Cr(NO_3)_3$	1600.56
$Fe(NO_3)_3{\cdot}9H_2O$	8887.56
$Eu(NO_3)_3{\cdot}5H_2O$	2996.28
Group 2—phosphate: $Na_3PO_4{\cdot}12H_2O$	4054.40
Group 3—sulfate: Na_2SO_4	7242.00
Group 4—fluoride: NaF	2813.33
Group 7—chloride: NaCl	1986.96

The bench-scale precipitation experimental setup was reported in details elsewhere [14]. For each of the six samples that were mixed with IPA, the formed inorganic precipitates were separated from the IPA-aqueous solution by vacuum filtration (Osmonics 0.2 μm dead-end filters). IPA was then condensed and recovered using a glass cold trap immersed in liquid nitrogen.

Five Dionex Ion Chromatography (IC) systems series-8200 were used for the analysis of inorganic species in the INEEL sodium-bearing liquid waste. Each of the five IC was equipped with advanced gradient pump (AGP-1), and automated sampler (AS40). The first IC, which was equipped

with a conductivity detector (CDM-III), was used for anions analysis. IonPac anion separation column (AS14A), IonPac anion guard column (AG14A), and anion self-regenerating suppressor (ASRS-Ultra) were employed. EPA method 300.1 was used as a guideline to determine the concentrations of anions [17].

The second IC was used for the analysis of the monovalent cations (sodium and potassium), divalent cations (calcium, strontium, and barium), and IPA. The IC was equipped with a conductivity detector (CDM-III), IonPac cation separation column (CS12A), IonPac cation guard column (CG12A), and cation self-regenerating suppressor (CSRS-Ultra). EPA method 300.7 [18] (as a guide) along with the Dionex Column Application Note [19] were used to determine the concentrations of such cations and IPA.

The third IC was used for the analysis of metals (iron, nickel, and manganese) and lanthanides (europium). The IC was equipped with a variable wavelength (UV/visible) detector (VDM-II). IonPac cation exchange column (CS5A) for the determination of metals and lanthanides with visible absorbance detection along with IonPac cation guard column (CG5A) were used. Dionex Application Note TN23 [20] was employed to perform the analysis of such species.

The fourth IC was used for the analysis of aluminum. The IC was equipped with a variable wavelength (UV/visible) detector (VDM-II), IonPac cation exchange column (CS2), and IonPac cation guard column (CG2). Dionex Application Note 42 [21] was used to determine the concentrations of aluminum.

The fifth IC was used for the analysis of chromium (III). This IC system was also equipped with a variable wavelength (UV/visible) detector (VDM-II). IonPac cation exchange column (CS5A) combined with IonPac cation guard column (CG5A) were used. Dionex Application Note TN26 [22] was employed for chromium analysis.

Calibration data (preparation of standards, serial dilution procedure, and IC consistency tests) were developed and described elsewhere [14,23]. The precipitation fractions (P) were calculated based on the determined concentrations of the targeted species in the reference sample (aqueous: $C_{1,2}$ or $x_{1,2}$), and the filtered samples (IPA-aqueous: $C_{1,m}$ or $x_{1,m}$) as follows [24]:

$$P = 1 - \frac{C_{1,m}}{C_{1,2}} = 1 - \frac{x_{1,m}}{x_{1,2}} \quad (1)$$

4. Presentation of the LPP experimental data

The LPP can be evaluated in terms of the precipitation fractions (P) as a function of the solvents volume ratio (V_r), that is the ratio of the IPA volume to the aqueous volume. The P values of aluminum (16,998 mg/L) and nitrate (117,180 mg/L) from the aluminum–nitrate system alone (concentrations as given in our simulated INEEL sodium-bearing liquid waste) over a V_r range extended from 0.025 to 0.8 were studied using IPA. As shown in Fig. 1, the P values of the aluminum were reached asymptotic values (%P: 99.9) at a V_r of 0.1, while

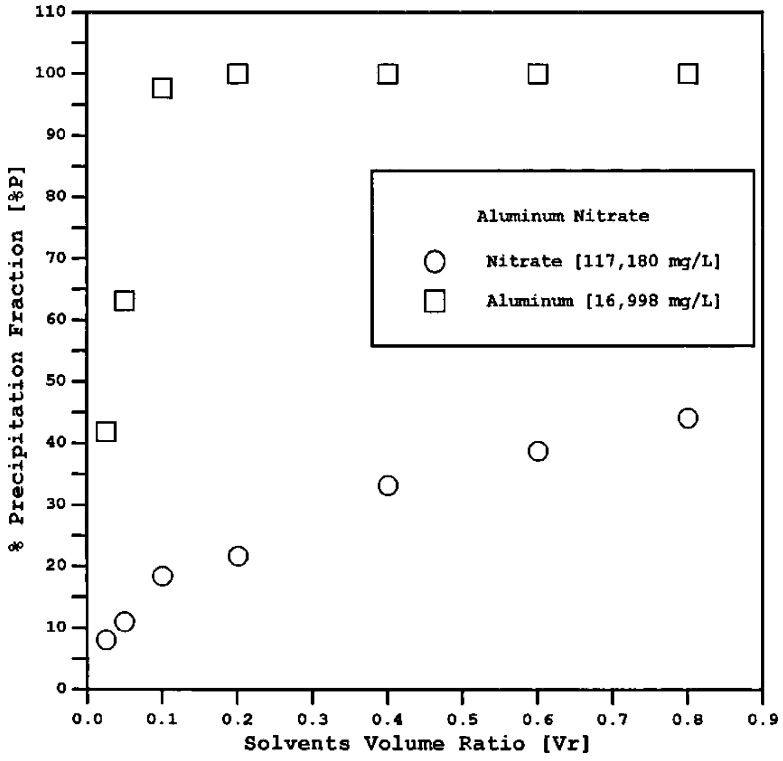

Fig. 1. Precipitation fractions for aluminum nitrate (INEEL sodium-bearing liquid stream).

the *P* values of the nitrate were significantly lower than the *P* values of the aluminum. However, the *P* values of the nitrate increased with the increase in the amount of IPA (5–45%). This indicates that aluminum nitrate decomposes in water to produce dissolved aluminum oxide and a basic nitrate in the form of nitric acid and some of the nitrate present as $Al(OH)(NO_3)_2$ [14].

It is worth noting that amorphous oxides such as aluminum oxide are generally sparingly soluble in water. However, the decomposition of nitrate in water in the form of nitric acid was substantially lowered the pH of the aqueous solutions (pH values were about 2.0), and thus kept the formed aluminum oxides dissolved in the aqueous solutions. Upon the addition of IPA, the aqueous solubility of aluminum oxide was drastically suppressed and aluminum was substantially precipitated. Hydrous oxide would fill the gap of the precipitated aluminum by forming a basic nitrate, which would lead to the low precipitation of nitrate. This preliminary data along with the chemistry of the INEEL sodium-bearing liquid waste strongly suggest that aluminum along with other polyvalent cations (metals, alkaline cations, and lanthanide) can effectively be precipitated in the form of oxides, while most nitrate in the forms of sodium and potassium will remain in the aqueous stream.

Fig. 2 shows the precipitation measurements for anions from the simulated INEEL sodium-bearing aqueous waste. The *P* values of fluoride and phosphate were very high (reached 99.9%). However, the *P* values of phosphate at the lower range of V_r were significantly lower (at $V_r = 0.025$, %*P*: 21.8 and at $V_r = 0.05$, %*P*: 84.6) than the *P* values of fluoride (at $V_r = 0.025$, %*P*: 99.5 and at $V_r = 0.05$, %*P*: 99.6). The *P* values of nitrate and chloride were relatively low, and were almost identical (at $V_r = 0.025$, %*P* for nitrate: 1.8 and for chloride: 2.4; and at $V_r = 0.8$, %*P* for nitrate: 41.4 and for chloride: 41.0). The *P* values of sulfate (%*P*: 10.5 at $V_r = 0.025$ and 65.5 at $V_r = 0.8$) were higher than the *P* values of nitrate and chloride but significantly lower than the *P* values of fluoride and phosphate.

Fig. 3 reveals that the *P* values of alkali cations (sodium and potassium) were low. As depicted in Fig. 4, the *P* values of sodium and potassium were comparable to the *P* values of nitrate and chloride. It should be pointed out that cesium was not included in the simulated INEEL sodium-bearing liquid waste. As documented earlier [14,23,25], the *P* values of cesium were generally about the *P* values of sodium and potassium. As such, the LPP process is, to some degree, ineffective in removing cesium. Fig. 3, however, shows that the *P* values of alkaline cations (calcium, strontium, and barium) were significantly high (reached asymptotic values, $P > 99.9\%$, at the V_r range of 0.2–0.8). Fig. 3 also reveals that the *P* values of the lanthanide (europium) were very high, and almost equivalent to the *P* values of alkaline cations.

Fig. 5 shows the *P* values of metals from the simulated INEEL sodium-bearing liquid waste. The *P* values of aluminum were very high (reached 99.9%), particularly, at the higher range of V_r (0.2–0.8). The *P* values of chromium (III) were constantly very high over the entire range of V_r. At the lower range of V_r (0.025 and 0.05), the *P* values of chromium were

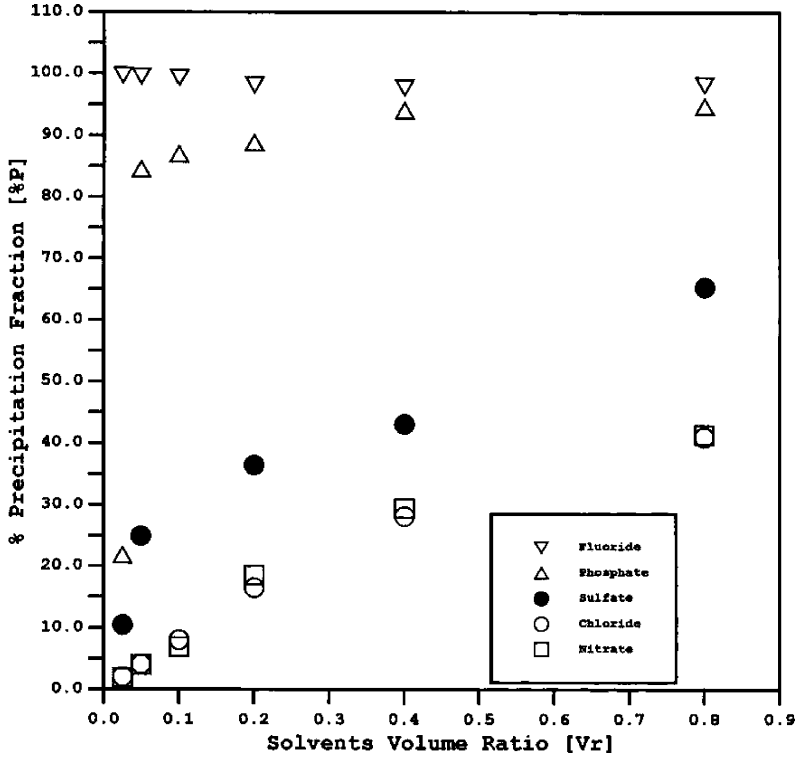

Fig. 2. Precipitation fraction for anions.

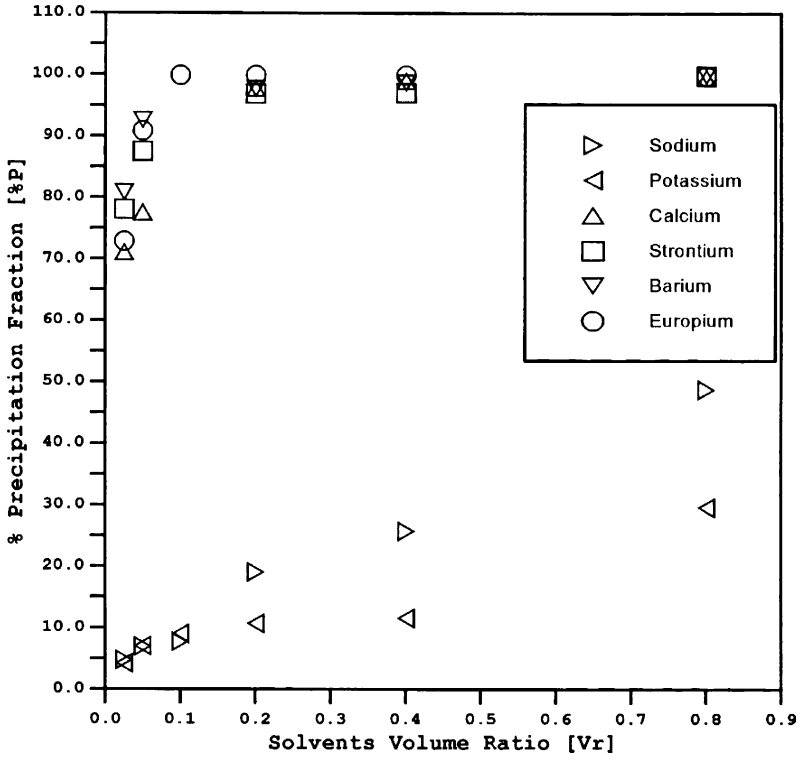

Fig. 3. Precipitation fractions for alkali cations, alkaline cations and lanthanide.

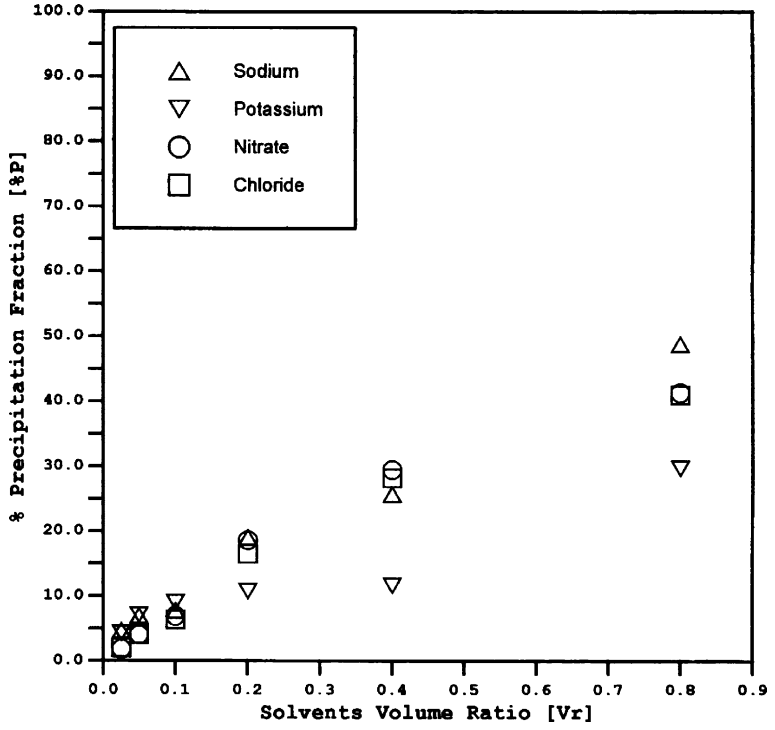

Fig. 4. Precipitation fractions for sodium, potassium, nitrate and chloride.

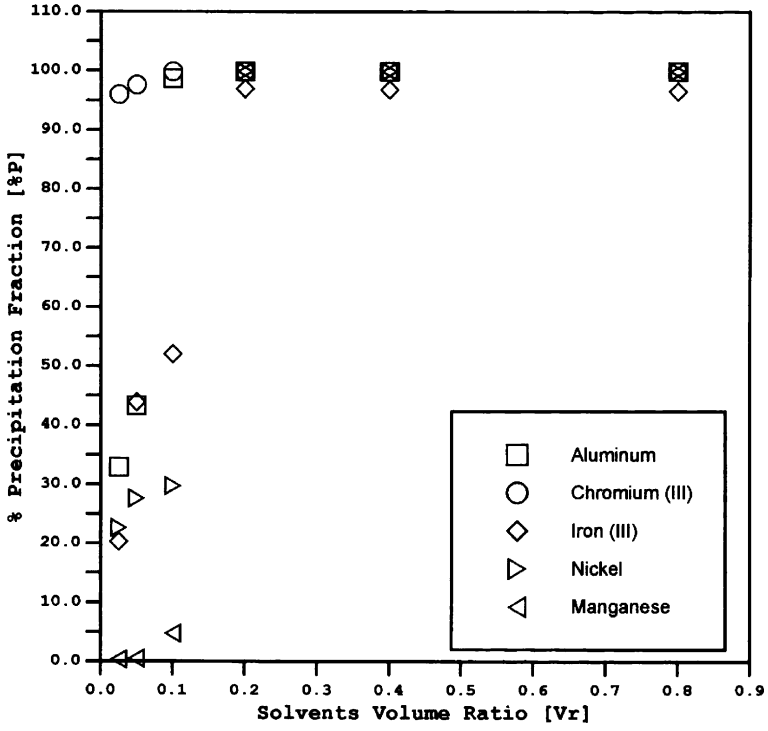

Fig. 5. Precipitation fractions for metals.

significantly higher than the P values of aluminum. The P values of iron (III) were lower than the P values of aluminum at the lower range of V_r (between 0.025 and 0.1), but were comparable to the P values of chromium and aluminum at the higher range of V_r (0.2–0.8). While the P values for the divalent metals (nickel and manganese) were significantly high at the higher range of V_r (0.2–0.8), they were very low, particularly manganese, at the lower range of V_r (0.025 and 0.1). It should be pointed out that mercury and lead as divalent metals were omitted from the simulated INEEL sodium-bearing liquid waste. However, such divalent species might exhibit precipitation trends similar to the precipitation trends of nickel and manganese.

Fig. 6 exhibits a comparison between the recovery of IPA from the INEEL sodium-bearing aqueous stream, and de-ionized water. A substantial recovery of IPA (98.5–99.7%) from the INEEL sodium-bearing aqueous was achieved compared to a moderate recovery from the de-ionized water (IPA: 47–94%) using a simple vacuum system. This indicates that the significant presence of inorganic species in the INEEL sodium-bearing aqueous stream along with the favorable physical properties of IPA have appreciably enhanced the removal of IPA from the aqueous phase.

5. Analysis of the LPP solid–liquid equilibrium model's equations

A framework derived from basic thermodynamic principles of solid–liquid equilibrium (SLE) criteria to correlate and predict the precipitation of inorganic species from aqueous solutions using organic solvents was developed [24]. The solubility (in terms of the activity coefficient) of a given inorganic species in a mixed-solvent mixture was related to the solubilities (in terms of the activity coefficients) of such a species in each of the pure solvents (water and IPA) using the excess Henry's constant approach. The Wohl's expansion [26] was then employed to model the excess Gibbs free energy (g^E) function. Two equations were provided; the 2-Suffix equation (two parameters: $x_{1,3}$ and Λ_{32}) [24]:

$$\ln[1-P] = \left[\frac{x_{1,m}}{x_{1,2}}\right] = \theta_3 \ln = \left[\frac{x_{1,3}}{x_{1,2}}\right] + \theta_2\theta_3\frac{v_1}{v_3}\Lambda_{32} \quad (2)$$

and the 3-Suffix equation (three parameters: $x_{1,3}$, Λ_{32} and Λ_{23}) [24]:

$$\ln[1-P] = \ln\left[\frac{x_{1,m}}{x_{1,2}}\right] = \theta_3 \ln\left[\frac{x_{1,3}}{x_{1,2}}\right] - \theta_2\theta_3[2\theta_3-1]\frac{v_1}{v_3}\Lambda_{32} + 2\theta_2\theta_3^2\frac{v_1}{v_2}\Lambda_{23} \quad (3)$$

where $x_{1,m}$ is the solubility of a given inorganic species in mixed-solvents media (water and IPA), $x_{1,2}$ the solubility of a given inorganic species in water solvent, $x_{1,3}$ the solubility of a given inorganic species in IPA, θ_3 the volume fraction of IPA, θ_2 the volume fraction of water, v_i the molar volume of species i (1: inorganic; 2: water; 3: IPA), and Λ_{32} and Λ_{23} are solvent–solvent (water–IPA) interaction parameters.

Regressions of the precipitation measurements were performed using the weighted least squares objective function

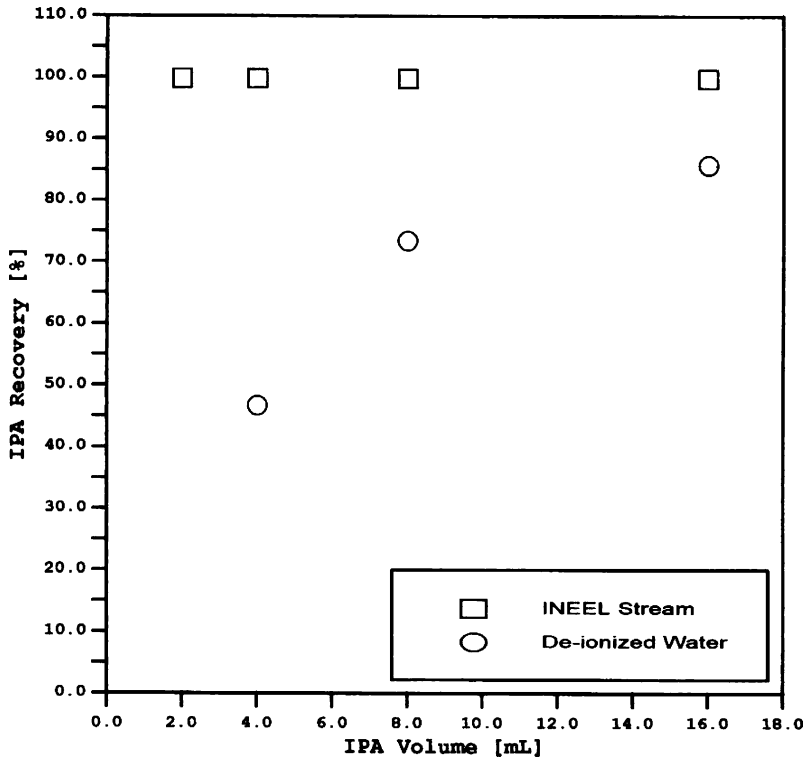

Fig. 6. Recovery of IPA from the simulated INEEL sodium-bearing stream and de-ionized water.

(SS). A Marquardt non-linear regression procedure was employed in the precipitation calculations [27]. The objective function, SS, used for the evaluation of the model equations is given as follows [24]:

$$\mathrm{SS} = \sum_{i=1}^{\mathrm{NP}} \left[\frac{Y_{\mathrm{Cal}} - Y_{\mathrm{Exp}}}{Y_{\mathrm{Exp}}} \right]^2 \tag{4}$$

where Y_{Cal} is the calculated variable, and Y_{Exp} the experimental variable, and given as follows [24]:

$$Y = \ln[1 - P] \tag{5}$$

According to Eq. (4), the root-mean-square-error (RMSE) provides an appropriate measure of the overall model performance for a given data set more so than the percentage average absolute deviation (%AAD) [24].

The acquired LPP data on the simulated INEEL sodium-bearing liquid waste were used to evaluate Eqs. (2) and (3). Table 2 summarizes the results of tested equations for the studied inorganic species. It should be pointed out that inorganic species with very high precipitation fractions (e.g., phosphate, fluoride, calcium, strontium, barium, cerium, europium, aluminum, and chromium) were removed. Eq. (2) with one solvent–solvent interaction parameter (Λ_{32}) provided in some cases acceptable correlation over the entire range of θ_3. When Eq. (3) with two solvent–solvent interaction parameters was used, however, a significant correlation improvement was accomplished. Such an improvement was attributed to the combination and asymmetric form of the solvent–solvent interaction parameters (Λ_{32} and Λ_{23}) with respect to θ_3.

Fig. 7 as an example exhibits a plot of the left-hand side of Eq. (2) or (3) versus the IPA volume fraction (θ_3) for the precipitation of sulfate from the INEEL sodium-bearing liquid waste. Without the addition of IPA, the left-hand side of these equations is zero since there is no precipitation ($P = 0$). Without the use of the solvent–solvent interaction parameters (Λ_{32} and/or Λ_{23}), the sulfate precipitation data can be fit to some extent with a straight line. This situation is equivalent to the ideal mixture solubility based on Henry's law. To extend the equations fittings to the maximum value of θ_3, the interaction parameters were needed to account for the non-ideality of the system. Eq. (2) with one regressed solvent–solvent interaction parameter (Λ_{32}) was insufficient to correlate the precipitation of sulfate over the entire range of θ_3 (RMSE = 0.1540; %AAD = 24.75). However, a significant correlation improvement was achieved with the use of Eq. (3) (RMSE = 0.0306; %AAD = 7.95).

Employing the regressed interaction parameters, Fig. 8 shows the experimental P values of sulfate from the INEEL sodium-bearing aqueous stream at different V_{r} values along with the predicted P values by Eqs. (2) and (3). The regressed parameters should provide economy of experimental efforts since they can be used: (1) to estimate the P values of the studied inorganic species at different concentration levels; or (2) for different waste streams with approximate abundance of major and minor inorganic species; or (3) at different solvents volume ratio (V_{r}) where no experimental data are available.

Table 2
The 2-Suffix equation (Eq. (2)) and the 3-Suffix equation (Eq. (3)) representations of inorganic species from the simulated INEEL sodium-bearing liquid waste

ME	Model's parameters			RMSE	%AAD	NP
	C_1	C_2	C_3			
Sodium ion						
Eq. (2)	−0.7965	−2.9751		0.0510	14.06	6
Eq. (3)	−7.3741	19.1492	8.4915	0.0089	4.95	6
Potassium ion						
Eq. (2)	0.4264	−2.6481		0.0835	39.93	6
Eq. (3)	−10.282	15.3601	7.1505	0.0139	12.26	6
Chloride ion						
Eq. (2)	−1.6729	4.3382		0.0144	10.94	6
Eq. (3)	−2.2913	7.3989	2.1627	0.0185	11.34	6
Nitrate ion						
Eq. (2)	−1.9927	3.5973		0.0535	13.37	6
Eq. (3)	2.8177	−10.7630	−5.0212	0.0363	10.74	6
Sulfate ion						
Eq. (2)	0.9650	−11.635		0.1540	24.75	5
Eq. (3)	−17.788	28.638	14.8573	0.0306	7.95	5

ME: model's equation; Eq. (2): $C_1 = \ln\frac{x_{1,3}}{x_{1,2}}$; $C_2 = \Lambda_{32}$; Eq. (3): $C_1 = \ln\frac{x_{1,3}}{x_{1,2}}$; $C_2 = \Lambda_{32}$; $C_3 = \Lambda_{23}$.

6. The LPP–MD hybrid technology

Based on the species profile of the INEEL sodium-bearing liquid waste, it appears that three main processing stages can be used to effectively treat the stream. The first stage targets the removal of the volatile nitric acid from the bulk of inorganic species by VMD. The second stage targets the separation of polyvalent cations (TRU elements, fission products, aluminum, chromium, phosphate, and fluoride) from the predominant bulk of monovalent anions and cations (mainly sodium nitrate) by a front-end LPP. The third stage targets the concentration of sodium nitrate by MD, and then

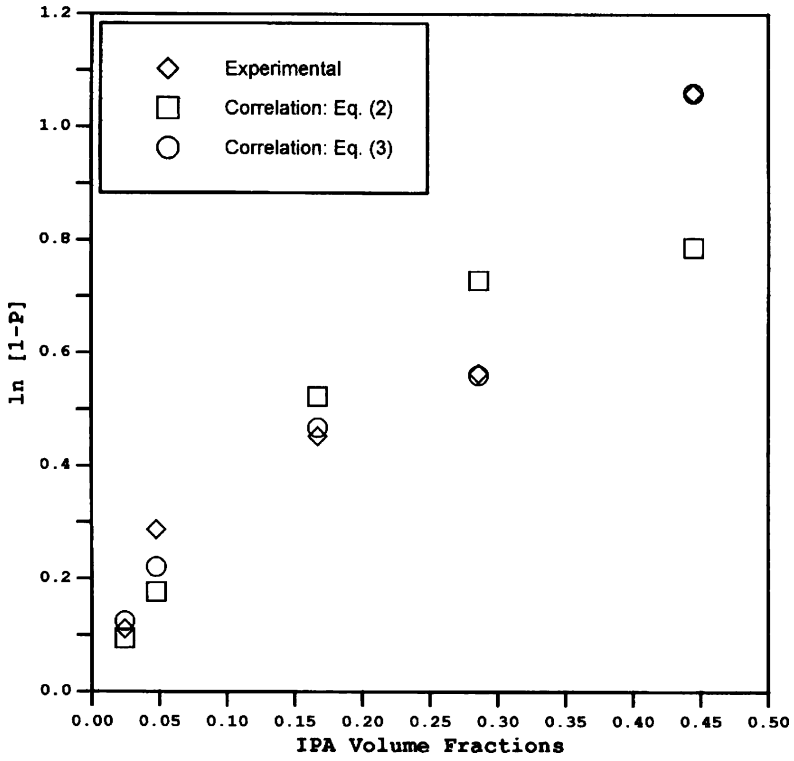

Fig. 7. Removal of sulphate from the INEEL sodium-bearing stream.

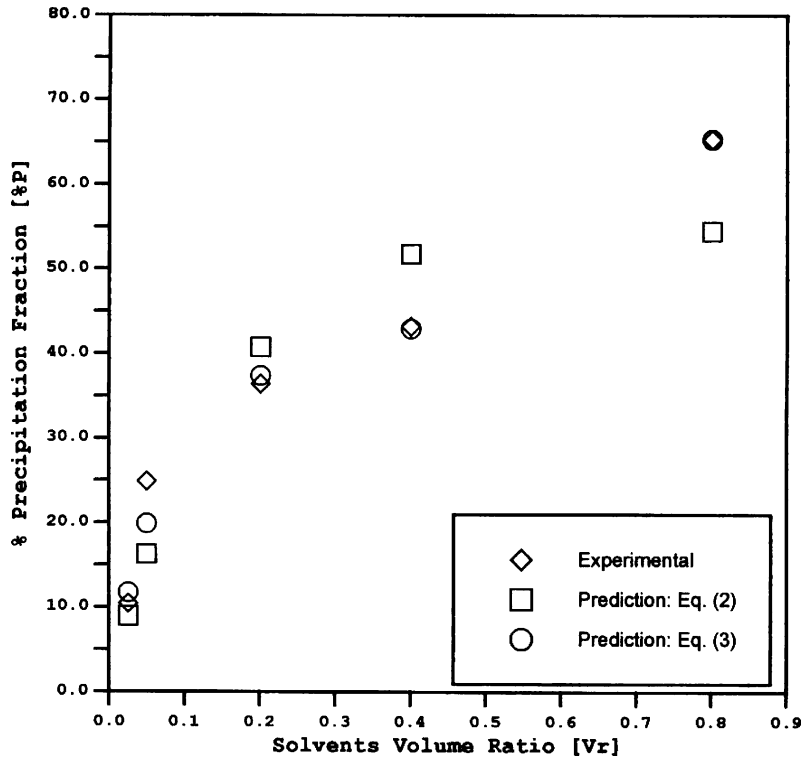

Fig. 8. Experimental and predicted precipitation fractions of sulphate from the INEEL sodium-bearing stream.

the separation of sodium nitrate from the aqueous phase by a rear-end LPP. Fig. 9 shows a simplified flow sheet for the hybrid LPP–MD system [28]. Following is a discussion about the integration of LPP–MD to achieve such processing stages.

6.1. Separation of nitric acid

As stated in the experimental section, the nitrate concentration in the INEEL sodium-bearing liquid waste was reduced from the reported value of 5.92–3.91 M to balance the total concentrations of anions against cations. As also indicated earlier, the INEEL sodium-bearing liquid waste is composed predominately of nitric acid and sodium nitrate. Nitric acid is completely dissociated to hydrogen and nitrate ions in aqueous stream. As such, the difference in the nitrate concentration (2.01 M) is attributed to the substantial existence of nitric acid. The simulated INEEL sodium-bearing liquid waste that was tested by the LPP step as given in the experimental section (with 3.91 M instead of 5.92 M of nitrate) was presumably free of nitric acid.

Fig. 10 shows the vapor pressures of nitric acid as a function of temperature [29]. VMD with or without some thermal gradient can be used as a pretreatment step for the front-end LPP to effectively remove and recover the volatile nitric acid from the INEEL sodium-bearing liquid waste. As shown in Fig. 9, the recovered nitric acid can be used, for instance, in future or simultaneous processing to dissolve and treat the stored high-activity calcined waste.

6.2. Separation of polyvalent cations from the bulk of dominant sodium nitrate

The precipitation data suggests that LPP is capable of segregating polyvalent toxic and radioactive cations from the bulk of monovalent anions and cations. Based on the preliminary LPP data of the simulated INEEL sodium-bearing liquid waste, the front-end LPP can be conducted in a single-stage at a V_r value of 0.1 to separate about 99.9% of calcium, strontium, barium, europium, aluminum and chromium; 99.5% of fluoride; 87% of phosphate; 53% of iron; 30% of sulfate; along with about 7% of sodium and potassium; and 6% of nitrate and chloride. The removal of such species in a single-stage front-end LPP will reduce the total inorganic concentration of the simulated INEEL sodium-bearing aqueous stream from 6.85 to about 5.63 M. The aim of such a single-stage LPP is the removal of the TRU elements and their fission products (except cesium), along with aluminum (the third largest species in the INEEL sodium-bearing waste), and other critical species such as chromium, phosphate and fluoride. This will allow the disposal of the remaining bulk of the INEEL sodium-bearing liquid waste as an LLW.

The definition of the US Nuclear Regulatory Commission (NRC) for the classes (A, B, and C) of LLW is given in Table 3 [30]. Reducing the radioactivity of the bulk of the INEEL sodium-bearing liquid waste to Class-A LLW is the targeted limit. To achieve such a limit, TRU elements, Sr-90, and Cs-137 must be removed, respectively, by 98.1, 99.98, and 99.5% [8]. It appears that the LPP is effectively capable

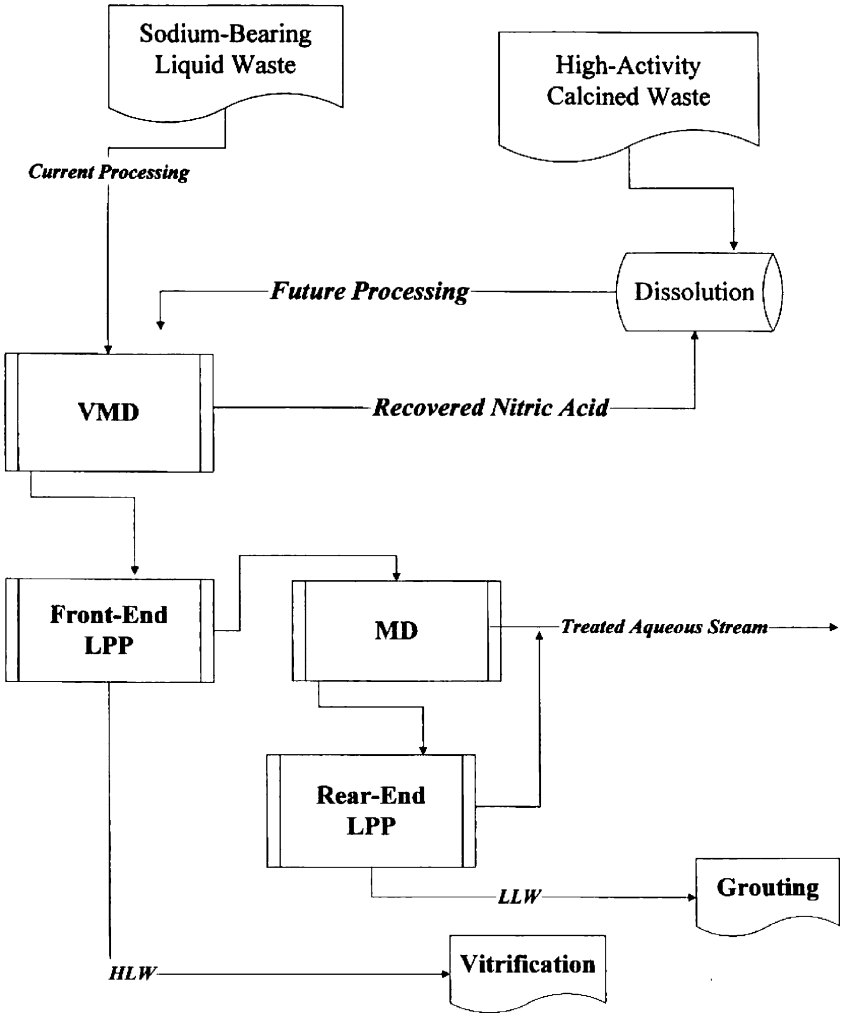

Fig. 9. A simplified flow sheet for the LPP–MD hybrid system to treat the INNEL acidic waste.

of removing TRU elements and strontium from the bulk of the waste to meet the definition of Class-A LLW.

A further benefit is the extraction of economic values from some of the precipitated species in the front-end LPP. For instance, the substantially precipitated aluminum (in the form of oxide) and/or phosphate (in the form of dilute sodium dibasic phosphate) can be reacted with magnesium oxide to form a stable ceramic (aluminum or phosphate or aluminum–phosphate bonded ceramic) [31]. Aluminum-based magnesium spinel ($MgAl_2O_4$) offers a desirable combination of properties including high melting point, high strength, high resistance to chemical attack, and high binding capability with nearly all elements, which could make it an important aluminum-based ceramic for the solidification and stabilization of HLW. Phosphate-based calcined magnesium ceramic are pore-free, insoluble in groundwater, stable at elevated temperatures, and capable of forming solid solutions with TRU and rare earth elements. Such bonded ceramics have the potential to accommodate a variety of DOE waste streams that are difficult (e.g., mixed-waste) to stabilize with current technologies. Zirconium (not yet tested by LPP), as a polyvalent cation, can effectively be precipitated by IPA in the form of oxide.

Table 3
Classifications of the US NRC low-level waste (LLW) [30]

	TRUs	SR-90	Cs-137
Class-A LLW	370 Bq/g	1480 Bq/mL	37000 Bq/mL
Class-B LLW	3700 Bq/g	5.55E6 Bq/mL	1.63E6 Bq/mL
Class-C LLW	3700 Bq/g	2.59E8 Bq/mL	1.70E8 Bq/mL

Bq: Becquerels.

At this time, however, vitrification is the most established and preferred method to immobilize HLW. Thus, there is always an interest to separate radioactive from non-radioactive species to reduce the cost of vitrification. TRU elements and their fission products could be segregated from aluminum if the single-stage front-end LPP is replaced by dual-stages. In the dual-stages LPP, the first stage can be conducted at a V_r value of 0.05 to remove about 90% of TRU elements and their fission products (except cesium); 99.8% of fluoride and chromium; 85% of phosphate; and 42% of aluminum. Precipitates from the first stage can be vitrified as an HLW. The

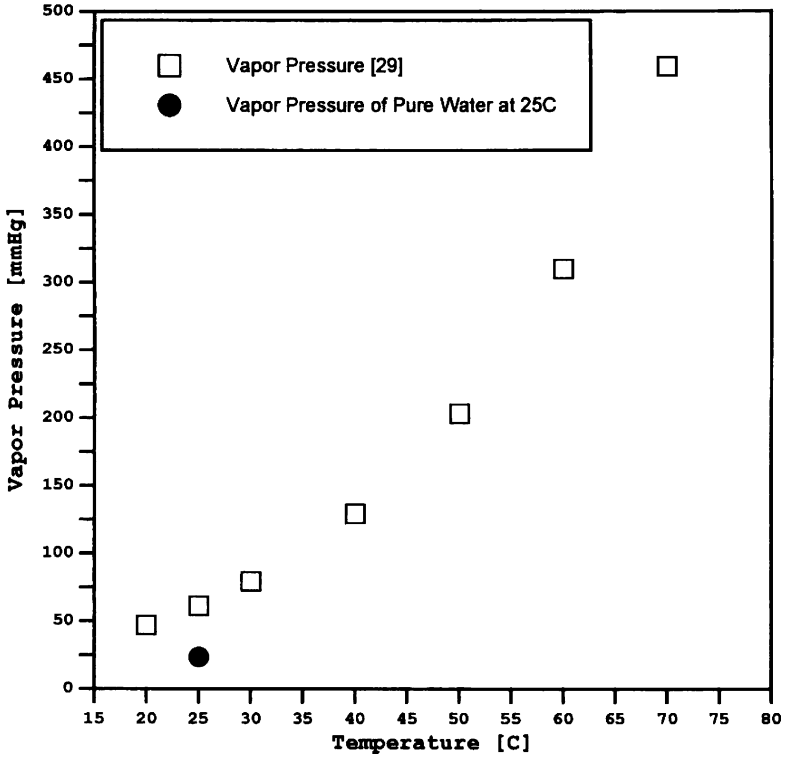

Fig. 10. Vapor pressures of nitric acid.

second stage will be conducted at a V_r value of 0.1 to remove aluminum along with the remaining TRU elements and their fission products, and some metals.

The overall performance of the dual-stages LPP in removing the targeted species will be equivalent to a single-stage LPP at a V_r value of 0.1. However, two factors would determine the use of a single-stage or dual-stages front-end LPP. The first and the most important factor is the cost saving in minimizing the operating cost of the vitrification process. The second factor is the operating cost of LPP (recovery and reuse of IPA) versus the capital cost of adding a second stage of LPP.

Fig. 11 depicts dual-stages front-end LPP. The filtration of the formed precipitates can be achieved by vapor-tight hydrocyclones (HC). The preliminary data indicate that the particle sizes of the formed precipitates are greater than 5 μm, which is the critical cut-off for HC. The preference of using HC is attributed to the their versatility, simplicity, low operating cost, and controllable underflow. With the design of HC multi-stages, the underflow for each stage can possibly be limited to approximately 5–10% of the feed.

The fundamental assumption in the design of the dual-stages LLP process is based on the changes in the chemical potentials in terms of measurable quantities such as temperature, pressure and composition [32]. At constant temperature and relatively low pressure, changing the amount of IPA, combined simultaneously with the change in inorganic concentrations due precipitation, will lead to changes in the phase equilibrium of the mixture. In the second stage of LPP, IPA will thus be added in a sufficient amount to compensate for the lost IPA in the first stage of the HC underflow, and to enhance the HC overflow from the first stage to reach a V_r value of 0.1. This assumption has been verified experimentally and found to be valid [33].

Thermodynamics vapor–liquid equilibrium calculations validated by experimental data indicated that IPA can nearly completely be recovered from aqueous solutions. Figs. 6 and 12 suggest the ease of IPA recovery. As such, VMD as a vapor–liquid equilibrium-based processing step would make a direct contribution to the recovery of IPA. Since the permeate flux in VMD is aided by a vacuum system, this may favor the wetting of the membrane pores in the feed side. For instance, if VMD is used in the LPP to recover IPA before the removal of precipitates by HC, then precipitates (depending on precipitates size) could fill the membrane pores and lead to rapid flux decline. As such, HC will be used before VMD to separate precipitates from the stream, and to protect the VMD membrane.

The overflow of the second stage of HC will be fed into a VMD unit to recover IPA. As shown in Fig. 11, each of the underflow streams from the HC stages will be fed into separate vacuum filter press units. The vacuum filter press units will be connected to the underflow VMD unit. The design of the HC underflow streams (vacuum filter press units and VMD) would serve the double objectives of: (1) separating and dehydrating precipitates in pure solid form (to be encapsulated for a final disposal or recovered as a commodity); and (2) recovering IPA from the HC underflow stream. The

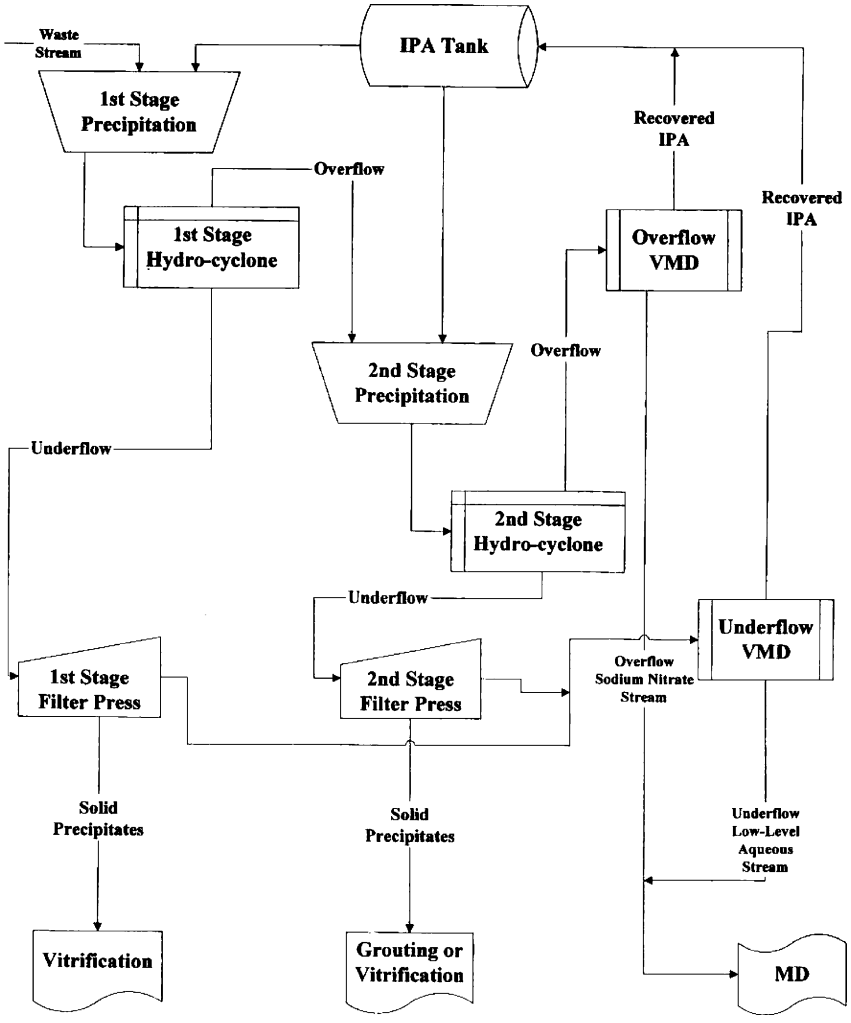

Fig. 11. A flow sheet for possible dual-stage front-end LPP.

recovered IPA from the HC overflow and underflow streams will be recycled for reuse. The dominantly sodium nitrate aqueous stream from the overflow VMD along with low-level aqueous stream from the underflow VMD will be fed into MD.

6.3. Separation of sodium nitrate

The osmotic pressure of the INEEL sodium-bearing liquid waste can simply be estimated by the following relation [34]:

$$\Pi = 1.19\,[T + 273.15] \sum M_i \tag{6}$$

Π is the osmotic pressure (psi), T the temperature (°C), and M_i the molar concentration of individual ions (mol/L). According to Eq. (6), the Π of the INEEL sodium-bearing liquid waste is 2756 psi at 25 °C. This would make, for instance, the application of pressure-driven membrane processes such as reverse osmosis to this stream practically impossible (the driving force is the difference between applied and osmotic pressures).

The vapor pressure of the aqueous stream can be related to the osmotic pressure and estimated by the following relation [35]:

$$p^{s} = \frac{p^{0}}{\exp\left[\Pi v_{w}/RT\right]} \tag{7}$$

where p^{s} is the vapor pressure of the aqueous solution (mmHg), p^{0} the vapor pressure of pure water (mmHg) at a given temperature, Π the osmotic pressure (psi) at a given temperature, v_w the water molar volume (L/gmol) at a given temperature, R the ideal gas constant (L psi/gmol K), and T the temperature (K).

If the front-end LPP is applied in a single-stage or dual-stages (as discussed above) to separate polyvalent toxic and radioactive cations from the bulk of monovalent anions and cations, the remaining INEEL sodium-bearing stream will contain about 94% of nitrate and chloride; 93% of sodium and potassium; and 70% of sulfate. The total concentration of the simulated INEEL sodium-bearing waste will be reduced by 18% (from 6.85 to 5.63 M). However, the concen-

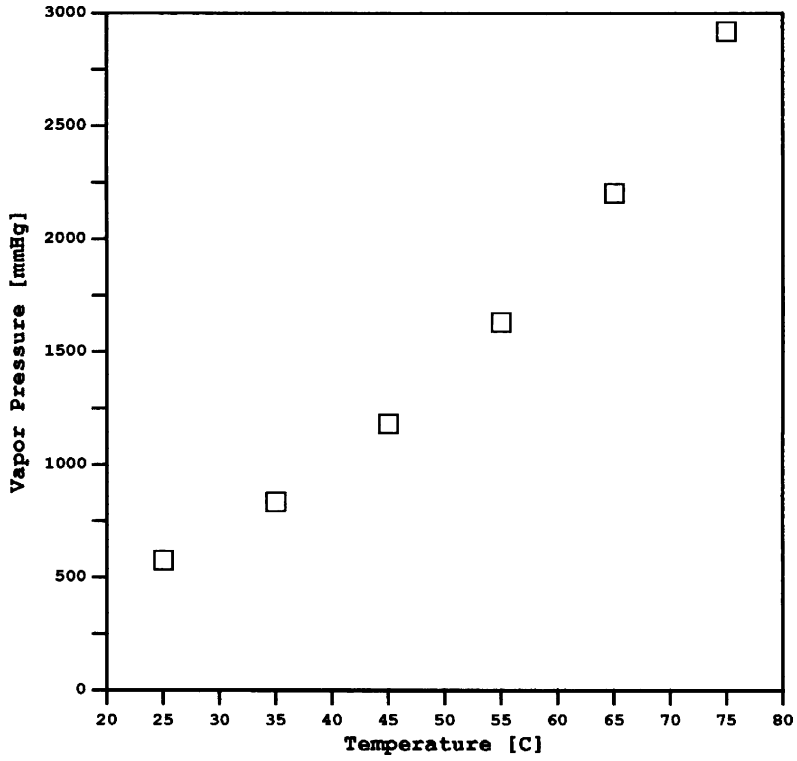

Fig. 12. Vapor pressure of IPA.

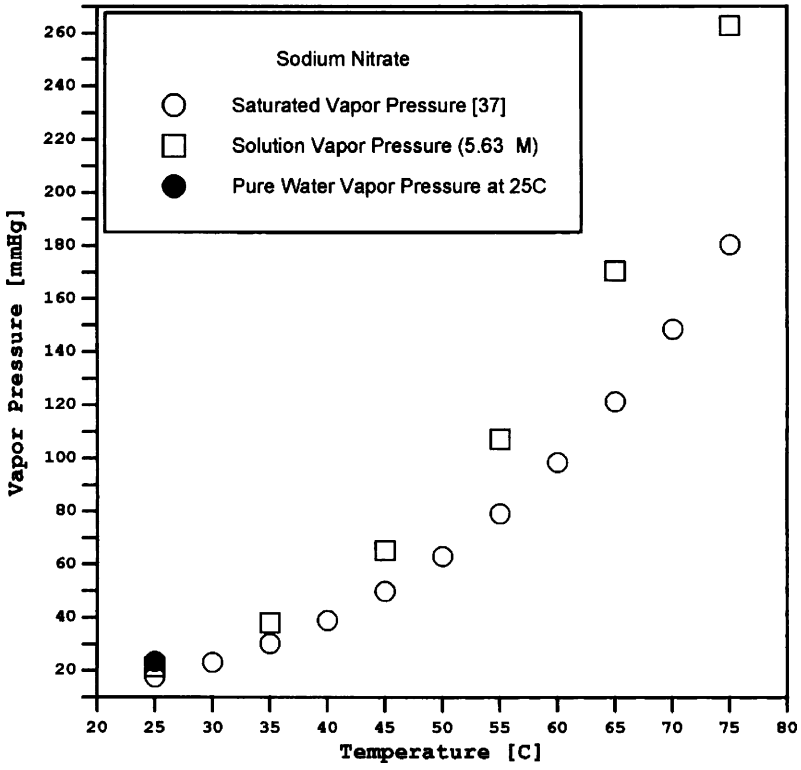

Fig. 13. Vapor pressures of sodium nitrate at saturation limits and solution concentration.

trations of chloride and sulfate are very marginal compared to the concentrations of nitrate and sodium. Nitrate is the dominant anion in the remaining INEEL sodium-bearing liquid waste. As such, the chemistry of the remaining INEEL sodium-bearing aqueous waste after the front-end LPP treatment can be reasonably approximated by the concentration of sodium nitrate.

Fig. 13 shows the vapor pressure of pure water at 25 °C (Antoine equation [36]), the vapor pressure of the remaining INEEL sodium-bearing aqueous waste (Eq. (7)), and the vapor pressure of the saturated sodium nitrate system [37] as a function of the MD operating temperatures range. The MD permeate stream is theoretically ultra-pure and the temperature of such a stream is typically 25 °C. If the temperature of the MD permeate is selected at 25 °C, then the vapor pressure of pure water at 25 °C is the limit, in which the vapor pressure of the MD feed stream should exceed. The MD permeate flux is proportional to the vapor pressure difference between the MD feed and permeate streams. Since the relation between the vapor pressure and temperature is exponential, it is expected that the relation between the MD flux and temperature is also exponential. As such, an increase or decrease in the MD flux depends on the temperature range of the feed rather than the temperature difference between the feed and permeate streams.

Fig. 14 exhibits the saturated concentrations of sodium nitrate at different temperatures [37]. The solubility limits of sodium nitrate are very high and temperature dependence (increase with increasing temperatures). In the targeted MD feed temperature range (45–75 °C), the saturation limits of sodium nitrate (15.47–19.97 M) are roughly about three-fold the concentration of the remaining INEEL sodium-bearing aqueous stream (5.63 M). As evaporation takes place in MD, the viscosity of the aqueous stream will increase with the increase of sodium nitrate concentrations. This would: (1) elevate osmotic pressures and depress vapor pressures; and (2) alter heat and mass transfer across boundary layers.

Fig. 15 shows that the elevation in the osmotic pressures at the saturation limits of sodium nitrate in the targeted temperature range (45–75 °C) is about three-fold higher than the osmotic pressures of the remaining INEEL sodium-bearing liquid waste. As shown in Fig. 16, however, vapor pressures at the saturation limits of sodium nitrate are slightly depressed (23–31%) from their values at the remaining concentrations (5.63 M) of the INEEL sodium-bearing aqueous stream. This indicates that MD permeate flux should not be greatly affected by the presence of significant concentration of sodium nitrate even at the saturation limit. MD is thus clearly capable of concentrating the remaining INEEL sodium-bearing aqueous stream to saturation without significantly affecting the driving force (higher vapor pressures in the feed stream than the permeate stream).

Effective operation of MD, however, demands controlling critical parameters such as temperature, feed concentration, and flow rate. Increasing viscosity, particularly for sodium nitrate with high aqueous solubility limits, could increase

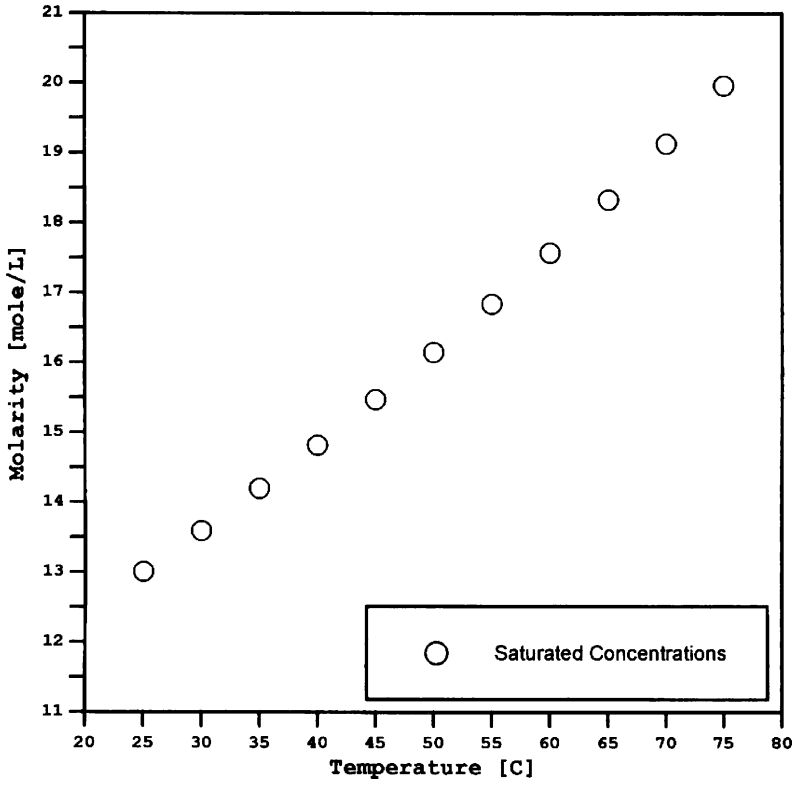

Fig. 14. The saturation limits of sodium nitrate.

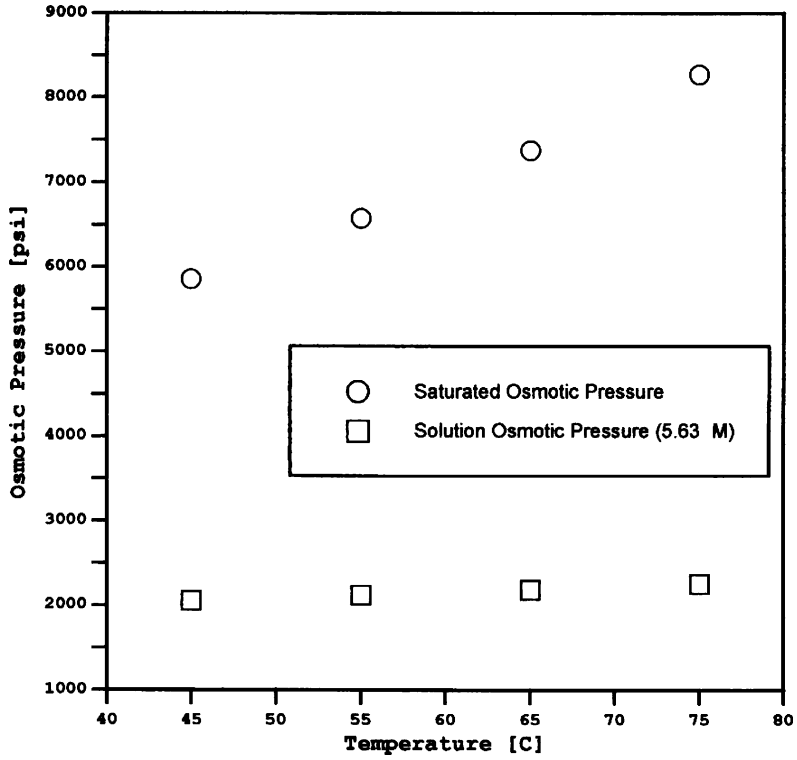

Fig. 15. Osmotic pressures of sodium nitrate at saturation limits and solution concentration.

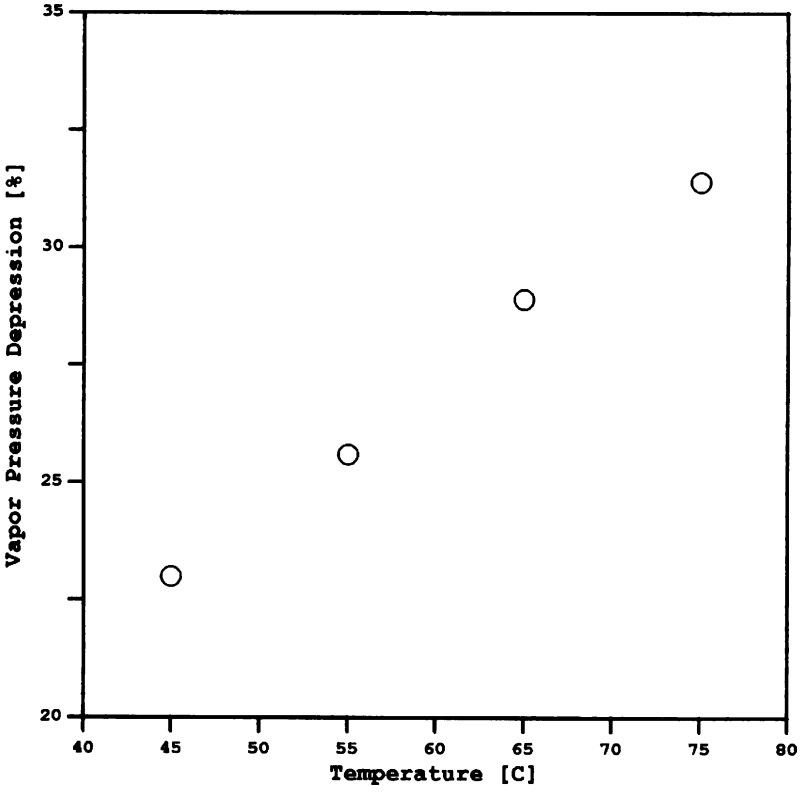

Fig. 16. Depression in vapor pressures between saturation limits and solution concentration (5.63 M) of sodium nitrate.

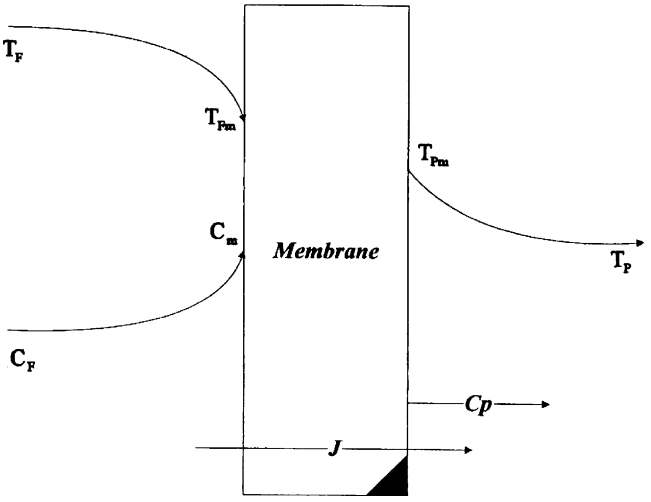

Fig. 17. Temperature and concentration profiles in MD.

boundary layer thickness, and thus could increase the overall resistance to heat and mass transfer at the membrane surface. This might have a greater effect on the permeate flux across the membrane. Temperature and concentration at the membrane surfaces could be substantially different from their values at the bulk streams. This could invoke the twin polarization phenomena in MD.

As depicted in Fig. 17, the bulk feed temperature (T_F) is higher than the feed temperature at the membrane surface (T_{Fm}), while the permeate temperature at the membrane surface (T_{Pm}) is higher than the bulk permeate temperature (T_P). Temperature polarization can take place on both sides of the membrane. However, it is more pronounced on the feed side than on the permeate side of the membrane. Heat is transferred in MD across the thin membrane and through the boundaries of the system by the latent heat of vaporization and conduction. Heat transfer by conduction, however, is a heat loss and a source of inefficiency. Hence, temperature polarization reduces the supply of heat for vaporization, enhances heat conduction, and limits mass transfer.

Fig. 17 also reveals that the bulk feed concentration (C_P) is lower than the concentration at the membrane surface (C_m). Concentration polarization could take place on the feed side of the MD membrane. Increasing concentration at the membrane surface will increase the osmotic pressure, and thus will decrease the vapor pressure. In addition, if MD is operated near saturation or at the saturation limit of sodium nitrate, then the solution viscosity would increase and precipitates would possibly be formed at the membrane surface resulting in spontaneous wetting of the membrane. Solution viscosity and membrane wettability could be the second important factor in declining MD permeate flux.

Flow rate influences both temperature and concentration at the membrane surface. Higher and optimum flow rates improve mixing conditions inside the MD module. In the case of temperature polarization, higher flow rates lead to minimize the difference between the bulk temperature and the temperature at the membrane surface on both sides of the membrane (feed and permeate). In the case of concentration polarization, higher flow rates could significantly minimize the concentration build-up at the membrane surface on the feed side. Thus, operating MD at optimum flow rates would make heat and mass transfer across the membrane more efficient.

MD should thus be operated below the saturation limit of sodium nitrate to prevent: (1) any decline in permeate flux; and (2) precipitates nucleation and build-up at the membrane surface. If the MD feed stream is conducted at 65 °C, then the concentration of sodium nitrate in the remaining INEEL sodium-bearing stream would fundamentally be concentrated by three-fold. This would: (1) increase the concentration from 5.63 to 16.89 M, which is below the saturation limit of sodium nitrate (18.34 M) at 65 °C; (2) minimize the influence of solution viscosity; and (3) eliminate membrane wettability on the feed side of MD. Once sodium nitrate is concentrated by MD to a level not detrimental to effective operation of MD, a single-stage rear-end LPP can then be used to induce effective precipitation of sodium (as well as potassium) nitrate for final disposal (or reuse).

It should be pointed out that remaining cesium can be co-precipitated with sodium nitrate. However, this may disqualify the disposal of the precipitated sodium nitrate as a Class-A LLW. Further studies are taking place to thoroughly evaluate the overall removal of cesium by the hybrid LPP–MD from the simulated INEEL sodium-bearing liquid waste. It should also be pointed out that several established ion exchangers are currently available for the removal of cesium from acidic waste streams [see e.g. 4–8]. A selected ion exchanger that exhibits a strong retention for cesium can be used before MD to remove the remaining cesium from the bulk of sodium nitrate.

7. Conclusions

The INEEL sodium-bearing liquid waste is dominantly concentrated with nitric acid and sodium nitrate. In addition, it contains aluminum (the third largest species) as well as toxic metals, and very small amounts of TRU elements and their fission products. As such, the hybrid LPP–MD is designed to treat the INEEL sodium-bearing liquid waste in three processing stages [28]. Each stage is focused on a certain type of species. The first stage will target the removal and recovery of nitric acid using VMD. The second stage will target mainly the removal of TRU elements and their fission products along with aluminum and some toxic metals for deep geologic and near-surface disposal facilities using a single-stage or dual-stages front-end LPP. The third stage will use: (1) MD to concentrate sodium nitrate to near saturation; and (2) a single-stage rear-end LPP to induce the precipitation and removal of sodium nitrate from the aqueous phase.

The approach of the LPP–MD hybrid system is similar to the pioneering work of the scientists at the Argonne National

Laboratory [38] and the INEEL facility [e.g. 4–8] in the sense of providing a so-called "full separation" approach, but is totally different in the processing concepts. In addition, the LPP–MD system could entirely eliminate the need for the calcination process. As such, the LPP–MD system could be a valuable addition to the DOE technologies toolbox.

Further benefits of the hybrid LPP–MD system are: (1) the extraction of economic values from the separated species; and (2) application for other waste streams across the DOE complex. For instance, the recovered nitric acid from the sodium-bearing liquid waste can be reused for future dissolving of the high-activity calcined waste. The precipitated aluminum in the form of oxide can also be reacted with magnesium oxide to form a stable ceramic for the solidification and stabilization of HLW or LLW. Once the high-activity calcined waste is re-processed and dissolved in nitric acid as planned, the LPP–MD hybrid system can also be applied to treat it.

References

[1] Tanks Focus Area, TFA—Multiyear Program Plan FY00-FY04, Appendix G—Description of DOE's Systems for Remediating Tank Waste, 2000.
[2] T.A. Todd, A.L. Olson, W.B. Palmer, J.H. Valentine, in: W.W. Schulz, N.J. Lomardo (Eds.), Science and Technology for Disposal of Radioactive Tank Wastes, Plenum Press, New York, 1998, pp. 35–43.
[3] Radioactive Tank Waste Remediation Focus Area, DOE/EM-0295, 1996.
[4] R.S. Herbst, J.D. Law, T.A. Todd, Sep. Sci. Technol. 37 (2002) 1321.
[5] J.D. Law, R.S. Herbst, T.A. Todd, Sep. Sci. Technol. 37 (2002) 1353.
[6] R.S. Herbst, J.D. Law, T.A. Todd, Sep. Sci. Technol. 37 (2002) 1807.
[7] N.R. Mann, T.A. Todd, Sep. Sci. Technol. 39 (2004) 2351.
[8] J.D. Law, K.N. Brewer, R.S. Herbst, T.A.D.J. Wood, Waste Manage. 19 (1999) 27.
[9] M.S.H. Bader, U.S. Patent 5,468,394 (1995).
[10] M.S.H. Bader, U.S. Patent 5,587,088 (1996).
[11] M.S.H. Bader, Separation of Salts, Scale Salts and NORM from Saline Solutions: Experimental and Modeling, Presented at the AIChE Summer National Meeting, Boston, August, 1995.
[12] M.S.H. Bader, Environ. Prog. 17 (1998) 126.
[13] M.S.H. Bader, J. Hazard. Mater. B 73 (2000) 269.
[14] M.S.H. Bader, J. Hazard. Mater. B 82 (2001) 139.
[15] M.S.H. Bader, U.S. Patent 6,365,051 (2002).
[16] M.S.H. Bader, U.S. Patent 6,663,778 (2003).
[17] J.W. O'Dell, J.D. Pfaff, M.E. Gales, G.D. Mcckee, Test Method: The Determination of Inorganic Anions in Water by Ion Chromatography, Method 300.0, EPA-600/4-84-017, March 1984.
[18] S.R. Bachman, J.E. Rothert, B. Kaiser, C.J. Brennan, M.E. Peden, Method 300.7—Dissolved Sodium, Ammonium, Potassium, Magnesium, and Calcium in Wet Deposition by Chemically Suppressed Ion Chromatography, EPA, March 1986.
[19] Installation Instructions and Troubleshooting Guide for IonPac CS12A Analytical Column and IonPac CG12A Guard Column, Dionex Technical Applications, 1999.
[20] Ion Chromatography of Lanthanide Metals, Dionex Technical Note TN23.
[21] Determination of Aluminum by Ion Chromatography, Dionex Application Note 42.
[22] Determination of Chromium in Water, Wastewater, and Solid Waste Extracts, Dionex Technical Note TN26.
[23] M.S.H. Bader, Selective Separation of Multiple Radioactive Contaminants from Liquid Waste Streams, BER/DOE, Bader Engineering and Research, Inc., 2000.
[24] M.S.H. Bader, J. Hazard. Mater. B 69 (1999) 319.
[25] M.S.H. Bader, Environ. Eng. Sci., submitted for publication.
[26] K. Wohl, Trans. AIChE 42 (1946) 215.
[27] D.W. Marquardt, J. Soc. Ind. Appl. Math. 11 (1963) 431.
[28] M.S.H. Bader, A Hybrid Technology for the Treatment of the INEEL Liquid and Calcined Waste, Patent Pending (2005).
[29] J.A. Duisman, S.A. Stern, J. Chem. Eng. Data 14 (1969) 457.
[30] US Nuclear Regulatory Commission, Licensing Requirements for Land Disposal of Radioactive Wastes, Code of Federal Regulations, Title 10, Part 61, 1994.
[31] M.S.H. Bader, Extraction of Aluminum from some of the INEEL Waste to Composite Stable Ceramic, Patent Pending (2005).
[32] M.S.H. Bader, J. Environ. Sci. Health A 29 (1994) 2139.
[33] M.S.H. Bader, Environmental issues and solutions in petroleum exploration, production, and refining, in: K.L. Sublette (Ed.), Proceedings of the Second International Petroleum Conference, New Orleans, PennWell Publishing Co., Oklahoma, 1995, pp. 717–727.
[34] A. Ko, D.B. Guy, in: P.S. Parekh (Ed.), Reverse Osmosis Technology: Applications for High-purity Water Production, Marcel Dekker, Inc, New York, 1988, pp. 189–193.
[35] D. Secrest, J. Chem. Educ. 73 (1996) 998.
[36] R.C. Reid, J.M. Prausnitz, B.E. Poling, The Properties of Gases and Liquids, 4th ed., McGraw-Hill, New York, 1987.
[37] D.G. Archer, J. Phys. Chem. Ref. Data 29 (2000) 1141.
[38] E.P. Horwitz, D.G. Kalina, H. Diamond, G.F. Vandegrift, W.W. Schulz, Solvent Extr. Ion. Exch. 3 (1985) 75.